

# Catalytic Wet Peroxide Oxidation of Phenol in Dark With Nanostructured Titania Catalysts: Effect of Exposure of Anatase 001 Plane

Michael Ferentz, Miron V.Landau\*, Roxana Vidruk-Nehemya, Moti Herskowitz

Department of Chemical Engineering, Blechner Center for Industrial Catalysis and Process Development, Ben-Gurion University of the Negev, Beer-Sheva, 84105, Israel  
 mlandau@bgu.ac.il

A series of nanocrystalline titanium oxide materials with anatase structure was collected by purchasing the commercial products and by solvothermal synthesis. Characterization of these materials by XRD, HRTEM and  $N_2$ -adsorption-desorption techniques showed that they displayed 10-30 nm crystal size, total surface area of 30-150  $m^2/g$  and the share of total surface area represented by [001] facets varied in range of 30-65%. The exposed surface of [001] facets in selected  $TiO_2$  materials varied in range of 9-94  $m^2/g$ . Testing of these materials as catalysts in catalytic wet peroxide oxidation of phenol revealed a strict correlation between the rate of phenol mineralization (conversion of TOC) and the value of exposed surface of [001] facets.

## 1. Introduction

Titanium oxide is known as efficient catalyst for photocatalytic degradation of organics in wastewater (Ananpattarachai et al., 2014; Busca et al., 2008). Recently was reported high efficiency of nanocrystalline titanium oxide (anatase) with surface area of 150  $m^2/g$  in catalytic wet peroxide oxidation (CWPO) of phenol in dark at low pH (Ferentz et al., 2015). This is the first application of  $TiO_2$  in organocatalytic  $H_2O_2$ -assisted water purification in dark. One of the directions for further improvements in this field is tailoring of the specific atomic configuration and associated surface reactivity of  $TiO_2$  nanocrystals by changing the relative exposure of their surface facets. The strong impact of this parameter on performance of  $TiO_2$  in photocatalytic reactions was well established in last decade and reviewed by Grabowska et al. (2014). The electronic properties of anatase  $TiO_2$  crystals with dominant [001] high-energy facets have a substantial effect on the surface separation and transfer of photo-generated electron-hole pairs determining the strong effect of these planes exposure in photocatalysis (Liu et al., 2011). The spontaneous dissociation of water molecules producing surface hydroxyls at adjacent Ti atoms bonded by a strong H bond is energetically favoured at [001] surface even in absence of light irradiation (Selloni, 2008). This is due to very high Ti-O-Ti bonds angles at this plane meaning destabilizing of O2p sites. Since formation of these adjacent H-bonded hydroxyls is the first step of catalytic  $H_2O_2$  decomposition to highly reactive  $\cdot OH$  radicals (Lousada et al., 2012) it was assumed that the exposure of [001] planes in anatase nanocrystals would favour also the organocatalytic activity of  $TiO_2$  in dark. Testing of this effect is the aim of the present work.

A series of anatase  $TiO_2$  materials consisting on truncated bipyramid nanocrystals of Wulff construction (Lazzeri et al., 2001) with crystal size 10-30 nm, surface area 30-150  $m^2/g$  and exposure of [001] planes 12-65% was tested in CWPO of phenol in a fixed-bed reactor in dark at 80°C. It was demonstrated that the first-order rate constant of phenol mineralization defined as TOC removal does not correlate with total surface area of catalytic materials but increases proportionally to the specific surface area of [001] planes in  $TiO_2$  nanocrystals. The estimated catalytic activity of [001] planes in anatase  $TiO_2$  nanocrystals was an order of magnitude higher compared with the activity of equivalent side [101, 011, 10 $\bar{1}$  and 01 $\bar{1}$ ] crystals facets.

## 2. Experimental

### 2.1 Preparation of titanium oxides

The titanium oxides were prepared by solvothermal method in presence (ST-TA) and absence (ST-NA) of diethylenetriamine (DETA) as crystallographic controlling agent. The isopropyl alcohol (>99.5%, Daejung), (DETA) (99.0%, Sigma-Aldrich) and titanium(IV) isopropoxide (>98.0%, Acros) used were of analytical grade. In a typical synthesis, 0.025ml of (DETA) was mixed with 28 ml of isopropyl alcohol and stirred for 3 min at room temperature, then 1 ml of titanium(IV)isopropoxide was dropped slowly into the above mixture. The resulting mixture was transferred into a Teflon-lined stainless autoclave (35 mL capacity). The autoclave was sealed and maintained at  $T=200\text{ }^{\circ}\text{C}$  for 24 h. The system was then allowed to cool ambient temperature. The final product was collected by centrifugation, washed thoroughly with ethanol, and dried at  $70\text{ }^{\circ}\text{C}$  overnight. The product was calcined at  $400\text{ }^{\circ}\text{C}$  for 2 h with a heating rate of  $1\text{ }^{\circ}\text{C min}^{-1}$ . Two commercial titanium oxides XT25384 (COM-II) and XT25376 (COM-I) were purchased from Saint-Gobain NorPro Co.

### 2.2 Characterization of titanium oxides

X-ray powder diffraction (XRD) patterns were recorded with a Philips 1050/70 powder diffractometer equipped with a graphite monochromator using software developed by Crystal Logic. The high resolution SEM and TEM micrographs were obtained using JSM 7400F scanning microscope and JEM 2010 transmission microscope at 200 kV. The  $\text{N}_2$ -adsorption-desorption Isotherms were obtained at the temperature of liquid nitrogen with a Surface Area & Pore Size Analyzer NOVA-3200e (Quantachrome) instrument.

### 2.3 Testing of catalysts performance

The catalytic activity of  $\text{TiO}_2$  materials was tested in CWPO of phenol as a model pollutant in water (200 ppm) at atmospheric pressure,  $\text{H}_2\text{O}_2/\text{PhOH} = 1.5$  (1520 ppmw of  $\text{H}_2\text{O}_2$  relative to stoichiometric demand for full PhOH conversion to  $\text{CO}_2/\text{H}_2\text{O}$ ), inlet pH = 2.5,  $T = 80\text{ }^{\circ}\text{C}$ , and water flow 4-40 cc/ g cat\*h in a tubular fixed-bed SS reactor with ID 7 mm (Ferentz, 2015). 0.10–0.25 mm catalysts particles were diluted with glass particles of 0.3–0.6 mm at volume ratio 1:1. The reactor was operated in an up-flow mode excluding liquid distribution problems. The TOC content in effluent water was analyzed using  $V_{\text{CPN}}\text{TOC}$  analyzer (Shimadzu Co.).

## 3. Results and discussion

According to XRD patterns (Fig. 1) all the  $\text{TiO}_2$  materials were pure titania phases with atomic order characteristic for anatase modification (Powder Diffraction File 4-784). Their average crystal size varied from 10 nm (ST-TA) to 30 nm (COM-II). The surface area varied from 30 to  $150\text{ m}^2/\text{g}$  with values of pore diameter and volume listed in Table 1.

Table 1: Texture parameters and crystal size of  $\text{TiO}_2$  materials

Sample	Surface Area (BET) [ $\text{m}^2/\text{g}$ ]	Pore Volume (Av.) [cc/g]	Pore Diameter (Av.) [nm]	Crystal Diameter (XRD) [nm]
ST-TA	145	0.45	12.4	10
ST-NA	65	0.15	4.5	20
COM-I	150	0.43	10.7	12
COM-II	30	0.17	20	30

According to HRTEM micrographs all  $\text{TiO}_2$  materials consisted of truncated bipyramid nanocrystals (Fig. 2) that at proper orientation yield rectangular or hexagon 2D images at the HRTEM micrographs. The calculation of the total theoretical surface area and exposure of [001] facets at the samples surface ( $\text{m}^2/\text{g}$ ) was conducted according to algorithm based on the amount of crystal unit cells placed in the nanocrystals volume and their width/height ratio  $N=a/b$  (Figure 2) assuming the theoretical density of anatase  $3.904\text{ g/cc}$ . The N value was established by statistical analysis of HRTEM micrographs taking in account crystals images with right hexagon shape. As shown in Fig. 3 the hexagons shape varied significantly causing change of N from 0.30 to 0.95 (Table 2). The surface area of exposed [001] facets varied from 9 to  $94\text{ m}^2/\text{g}$  corresponding to their relative exposure in individual nanocrystals from 30 to 55% (Table 2). Elongated flat nanocrystals obtained in

presence of amine crystallographic controlling agent (ST-TA, Fig.3.1) displayed maximal exposed surface of [001] planes while the COM-II material (Fig.3.3) demonstrated the lowest exposed surface of [001] facets. Since the nanocrystals formed aggregates with different types of connectivity, the estimation of the exposure of [001] facets requires corrections taking into account the self-screening of crystallographic planes in aggregates. In the ST-TA material the primary nanocrystals were connected in particle-linked nanowires packed in microspheres (Fig.4.1).

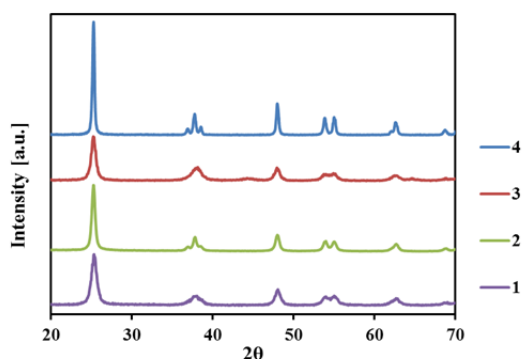


Figure 1: XRD patterns of  $\text{TiO}_2$  materials: 1-ST-TA; 2- ST-NA; 3- COM-I; 4 – COM-

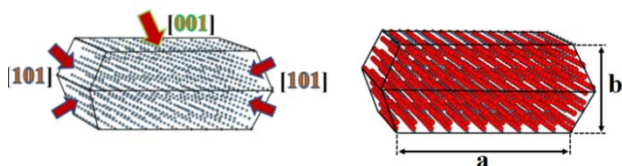


Figure 2: Schematic representation of bipyramid  $\text{TiO}_2$  nanocrystals: left- only Ti atoms; right – oxygens layers

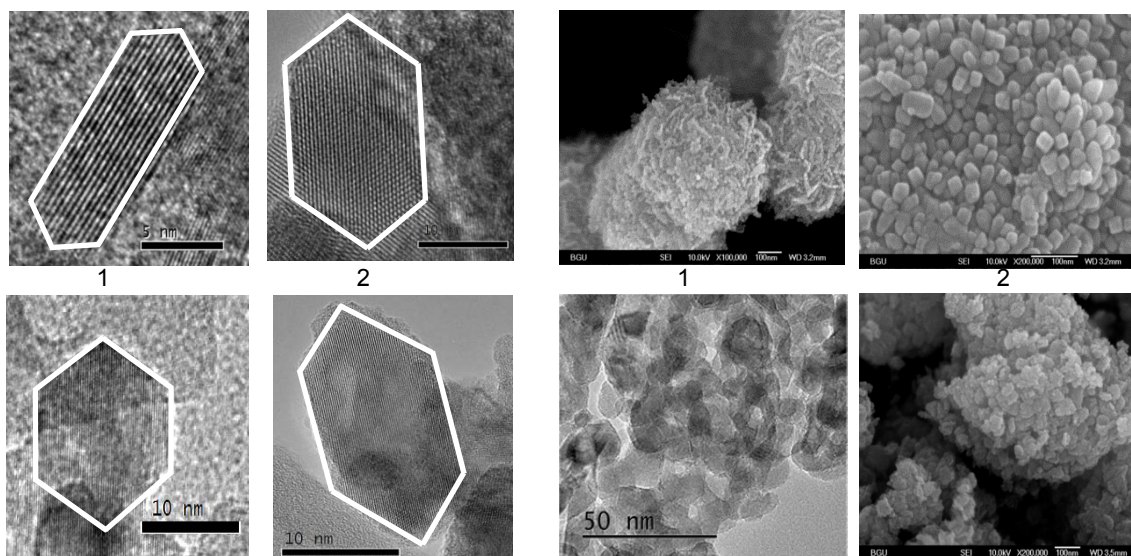


Figure 3: HRTEM images of individual nanocrystals in  $\text{TiO}_2$  materials: 1 - ST-TA; 2 - ST-NA; 3 – COM-I; 4 – COM-II

Figure 4: Aggregates of individual nanocrystals in  $\text{TiO}_2$  materials: 1 - ST-TA; 2 - ST-NA; 3 – COM-I; 4 -COM-II

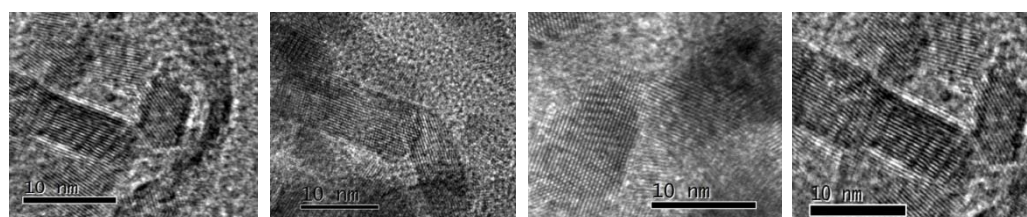


Figure 5: Association spaces of nanocrystals in nanowires of ST-TA  $\text{TiO}_2$  material

Table 2: Exposure of [001] facets in TiO<sub>2</sub> materials and rate constants of phenol mineralization in CWPO

Sample	S.A. (BET) m <sup>2</sup> /g	N=a/b	S.A.Theor. [m <sup>2</sup> /g]					$\psi$	Exposed [001] m <sup>2</sup> /g	K <sub>w</sub> g <sup>-1</sup> ·h <sup>-1</sup> ·cm <sup>3</sup>	K <sub>w</sub> heterog.= K <sub>w</sub> -K <sub>blank</sub> g <sup>-1</sup> ·h <sup>-1</sup> ·cm <sup>3</sup>
			S <sub>Total</sub>	S <sub>001</sub>	S <sub>101</sub>	[001] facets %					
						crystals	aggregates				
ST-TA	145	0.30	171	94	77	55	65	1.18	94	16	15.2
ST-NA	65	0.50	79	30	49	38	38	1.21	25	9	8.2
COM-I	150	0.95	150	18	132	12	12	1.00	18	4.5	3.7
COM-II	30	0.61	50	17	33	30	30	1.66	9	3.3	2.5

In other materials nanocrystals, aggregates did not show a specific orientation (Fig.4.2-4). The effect of self-screening of crystallographic planes in nanocrystalline aggregates on their exposed surface area may be estimated by the aggregation ratio  $\psi$ , calculated as S.A.theor./S.A.BET which is the ratio between calculated theoretical surface area of individual nanocrystal and actual exposed surface area measured by BET method (Landau, 2014). The  $\psi$  values presented in Table 2 show that in COM-I material the primary nanocrystals are not screening each other ( $\psi = 1.00$ ). In other materials this value varied from 1.18 to 1.66. This means that in COM-I TiO<sub>2</sub> the relative exposure of [001] facets is equal in nanocrystals and their aggregates. The surface area of [001] facets displayed in materials ST-NA and COM-II with random orientation of nanocrystals may be calculated as S.A.[001] aggregates = S.A.[001]theor./ $\psi$ .

In case of ST-TA material for calculation of [001] planes exposure should be taken in account the specific connectivity of primary nanocrystals in nanowires. It is very difficult to find on HRTEM micrographs images nanowires where primary particles are oriented relative to the electronic beam so as to detect the fringes of atomic layers in all the nanocrystals. Therefore the micrographs areas were carefully considered so the atomic structure of nanocrystals may be seen in two adjusted crystallites (Fig.5). The primary nanocrystals were connected by their side [101] planes leaving [001] facets exposed. The fringes of atomic layers corresponded to [101] planes with spacing of 0.352 nm are cut at the contact interface. It means that elongated TiO<sub>2</sub> nanocrystals in ST-TA material forming nanowires are not connected through coupling of their [001] facets. In this case, the fringes of atomic layers in two neighbouring crystallites are extended from one nanocrystal to another without changing the direction (Fig.2). These considerations were the basis for building a model of nanocrystals connectivity in nanowires of ST-TA material shown in Figure 6. This type of connectivity may be realized assuming preferential adsorption of DETA as crystallographic controlling agent at the [001] planes of growing TiO<sub>2</sub> crystals. Selective adsorption of amine molecules on [001] planes not only favours the crystals

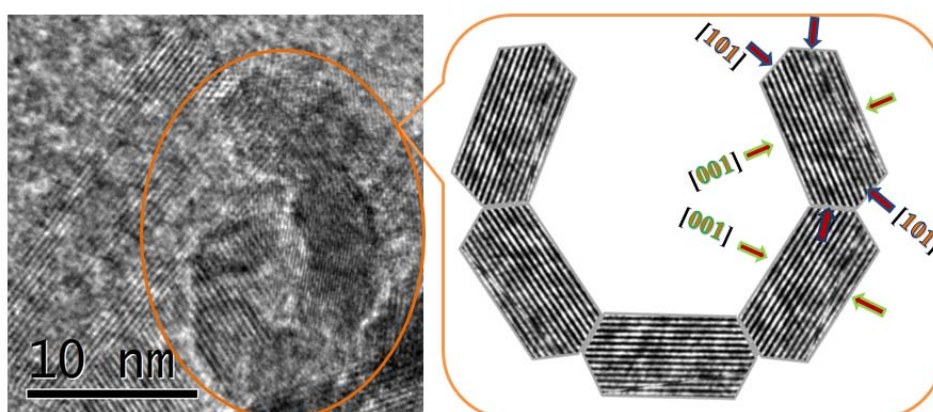


Figure 6: HRTEM image of particle-linked nanowire in ST-TA TiO<sub>2</sub> and schematic representation of their aggregation mode

growth in direction increasing the exposure of these planes in individual nanocrystals (Zhang, 2009) but also protects these facets from coupling during aggregation. Based on the above considerations, the relative exposure of [001] facets in nanowires of ST-TA TiO<sub>2</sub> should be higher than its theoretical value calculated for individual nanocrystals by the  $\psi$  factor. The aggregation increases the share of [001] facets in exposed total surface area from the theoretical value of 55% to 65% (Table 2). The last number (65%) was used for calculation of physically exposed [001] surface (m<sup>2</sup>/g) in ST-TA material (Table 2) that is equal to its theoretical value since [001] planes are not screened.

Measuring the conversion as a function of residence time for the four selected TiO<sub>2</sub> materials in CWPO of phenol indicated a first-order equation reaction.  $\ln(1-X_{\text{TOC}})$  plotted as a function of  $W/Q$ , where  $X_{\text{TOC}}$  – conversion of total organic carbon,  $W$  – weight of catalyst loaded to reactor (g),  $Q$  - flow rate of aqueous phenol solution (cc/h) (Fig.7) yielded a linear dependency where the slope  $k$  is the rate constant ( $\text{g}_{\text{cat}}^{-1} \cdot \text{h}^{-1} \cdot \text{cc}$  solution). According to the values of calculated rate constants of phenol mineralization the catalytic activity of tested materials increased in the sequence: ST-TA > ST-NA > COM-I > COM-II (Table 2). The blank testing experiment conducted at the same conditions in a reactor loaded with glass particles yielded TOC conversions corresponding to the equivalent value of the reaction rate constant of  $0.8 \text{ g}_{\text{cat}}^{-1} \cdot \text{h}^{-1} \cdot \text{cc}$  solution. Subtracting this value from the measured rate constants represents the heterogeneous catalytic reaction rates (Table 2). In absence of diffusion limitations excluded by implementation of small 0.10-0.25 mm catalysts particles the catalytic activity is determined by the TiO<sub>2</sub> surface area multiplied with the value of specific reaction rate constant:  $k = k_s \cdot \text{S.A.}$  Assuming that the specific catalytic activity (per 1 m<sup>2</sup> of solid) is constant for all the materials depending only on their chemical composition - TiO<sub>2</sub>, the kinetic rate constants of all materials should be proportional to their total surface area.

Plotting the measured rate constants vs the total surface area of tested materials (Fig.8.1) does not show a linear correlation. However, the plot in Fig.8.2 indicates that the catalytic activity of TiO<sub>2</sub> materials correlates well with the exposed surface area of active [001] facets in nanocrystalline aggregates. Extrapolation of graph presented in Fig.8.2 to the  $\text{S.A.}_{[001]} = 150 \text{ m}^2/\text{g}$  assuming that all the total surface in COM-I or ST-TA materials is represented by [001] facets yields the rate constant value  $k \sim 25 \text{ g}_{\text{cat}}^{-1} \cdot \text{h}^{-1} \cdot \text{cc}$  solution. Extrapolation to the opposite direction assuming that the total surface is represented by [101] facets gives the rate constant value of  $k \sim 2.5 \text{ g}_{\text{cat}}^{-1} \cdot \text{h}^{-1} \cdot \text{cc}$  solution. Therefore, the catalytic activity of [001] facets of TiO<sub>2</sub> anatase nanocrystals in CWPO oxidation of phenol is an order of magnitude higher compared with activity of [101] facets. As mentioned above this may be a direct consequence of high Ti-O-Ti bonds angles at [001] surface plane meaning destabilizing of O2p sites and leading to spontaneous dissociation of water molecules and producing surface hydroxyls at adjacent Ti atoms (Selloni, 2008). Formation of such surface hydroxyl pairs is critical for selective decomposition of H<sub>2</sub>O<sub>2</sub> into ·OH radicals highly reactive in phenol oxidation (Lousada et al., 2012).

The presented data suggest further improvement of TiO<sub>2</sub>-based catalysts for CWPO of organic contaminants in water requires increasing the exposure of [001] facets of anatase nanocrystals to more than 80%. This means preparation of thin nano-sheets of TiO<sub>2</sub> with high exposure of [001] planes on both sides. Preparation and stabilization of such nano-sheets is a challenge, since they curve and aggregate. Application of TiO<sub>2</sub> anatase nanotubes with [001] planes exposed at their inner and external surface is another challenge.

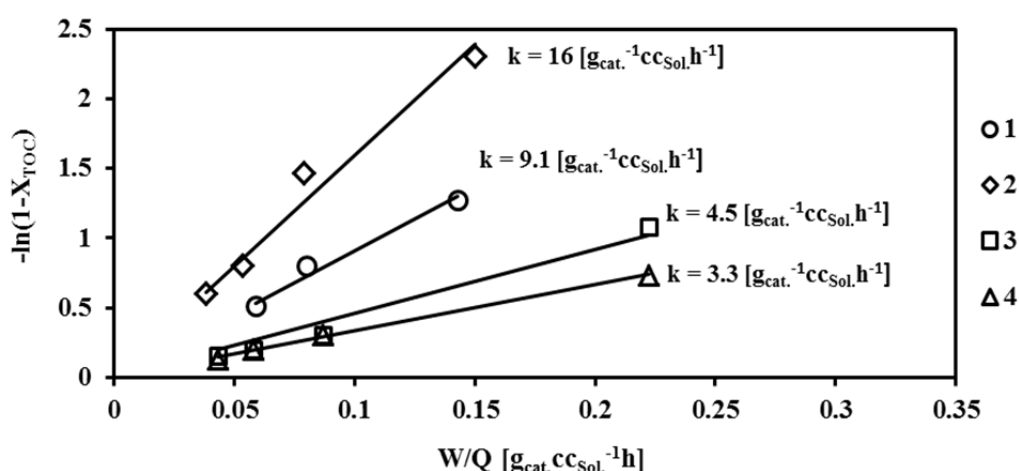


Figure 7: Kinetics of phenol mineralization by CWPO with following catalytic materials: 1 – ST-NA; 2 – ST-TA; 3 – COM-I; 4 – COM-II

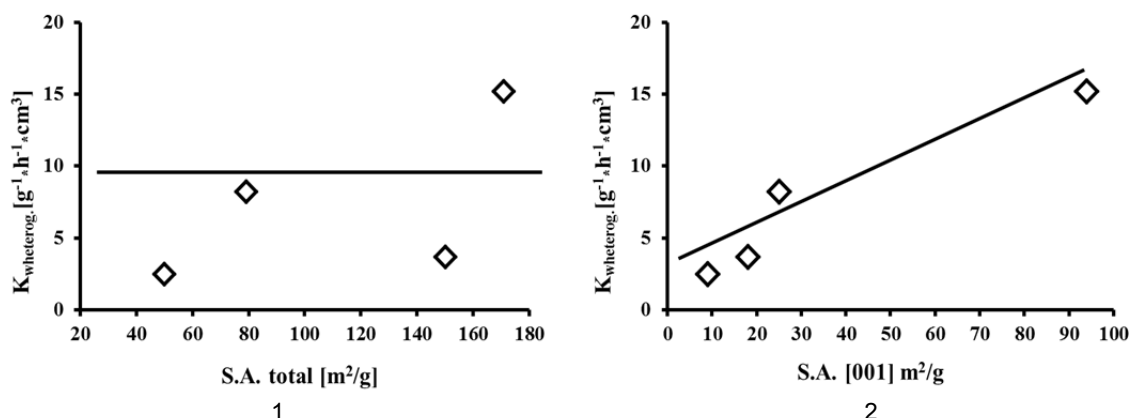


Figure 8: Correlations between phenol mineralization rate constants and catalysts surface area: 1 – total surface area; 2 - surface area of exposed [001] crystal planes of TiO<sub>2</sub> materials\

#### 4. Conclusions

The exposure of high-energy [001] facets in anatase nanocrystals with Wulff construction of truncated bipyramid determines their catalytic activity in phenol CWPO in dark. This may be attributed to spontaneous water dissociation being a sequence of unique atomic configuration at the surface of [001] crystal planes and leading to formation of surface hydroxyl pairs directing the H<sub>2</sub>O<sub>2</sub> decomposition to ·OH radicals.

#### Acknowledgments

We acknowledge the financial support provided by Ben Gurion University of the Negev in the framework of the collaboration between BGU, the Institute for Molecular Engineering at the University of Chicago, and Argonne National Laboratory on the Engineering and Science of Water Resources. The authors are grateful to Dr. A. Erenburg and Dr. V. Ezersky for characterization of catalysts using XRD and HRTEM methods, respectively.

#### References

- Ananpattarachai J., Kajitvchyanukul P., 2014, Adsorption and Degradation of 2-Chlorophenol by TiO<sub>2</sub>/AC and TiO<sub>2</sub>/CB in Photocatalytic Process, Chem.Eng.Transactions, 42, 157-162.
- Busca G. Berardinelli S., Resini C., Arrighi L., 2008, Technologies for the removal of phenol from fluid streams: a short review of recent developments, J.Hazard.Mater., 160, 265-288.
- Ferentz M., Landau M.V., Vidruk R., Herskowitz M., 2015, Fixed-bed catalytic wet oxidation of phenol with titania and Au/titania catalysts in dark, Catal. Today, 241A, 63-72.
- Grabowska E., Dial M., Marchelek M., Zaleska A., 2014, Decahedral TiO<sub>2</sub> with exposed facets: Synthesis, properties, photoactivity and applications, Appl.Catal. B: Environmental, 156-157, 213-235.
- Landau M.V., Vidruk R., Vingurt D., Fuks D., Herskowitz M., Grain boundaries in nanocrystalline catalytic materials as a source of surface chemical functionality, Rev.Chem.Eng.,30, 379-401.
- Lazzeri M, Vittadini, Selloni A., 2001, Structure and energetics of stoichiometric TiO<sub>2</sub> anatase surfaces, Phys.Rev. B 63, 155509-1-9.
- Liu S., Yu J., Jaroniec M., 2011, Anatase TiO<sub>2</sub> with Dominant High-energy [001] Facets: Synthesis, Properties and Applications, Chem.Mater. 23, 4085-4093.
- Lousada C.M., Johansson, A.J., Brinck M., Jonsson M., 2012, Mechanism of H<sub>2</sub>O<sub>2</sub> decomposition on Transition Metal Oxide Surfaces, J.Phys.Chem.C, 116, 9533-9543.
- Selloni A., 2008, Anatase shows its reactive side, Nature Materials, 7, 613-615.
- Zhang D., Li G., Yang X., Yu J.C., 2009, A micrometer size TiO<sub>2</sub> single-crystal photocatalyst with remarkable 80% level of reactive facets, Chem.Commun. 4381-4383.